JOURNAL OF MATERIALS SCIENCE 25 (1990) 1261–1267

The influence of process parameters and starting composition on the carbothermal production of sialon

E. KOKMEIJER, C. SCHOLTE, F. BLÖMER, R. METSELAAR
Centre for Technical Ceramics, P.O. Box 513, 5600 MB Eindhoven, The Netherlands

The β'-sialons ($Si_{6-z}Al_zO_zN_{8-z}$) can be produced by carbothermal reduction of kaolin. The reaction mechanism of the sialon formation has been studied by several methods. Firstly, the composition of the reaction product is determined by XRD as function of the reaction time at 1400 and 1500° C. The influence of additives, pellet size, nitrogen flow and clay type on the reaction is studied. Secondly, the carbon monoxide leaving the furnace is monitored. By studying the changes in carbon monoxide output as a function of the above-mentioned parameters a better understanding of the reaction mechanism has been obtained.

1. Introduction

The production of β'-sialon ($Si_{6-z}Al_zO_zN_{8-z}$) with $z = 3$ from kaolinite and carbon is given by the overall reaction:

$$3(2SiO_2 \cdot Al_2O_3 \cdot 2H_2O) + 15C + 5N_2 \rightarrow 2Si_3Al_3O_3N_5 + 15CO + 6H_2O \qquad (1)$$

This reaction is schematically represented by the dotted line in the phase diagram in Fig. 1 [1].

The overall Reaction 1 can be separated in several stages. During the first stage the crystal water will be removed from the kaolin at 560° C. Thereafter, at 960° C, the *meta*-kaolin dissociates into mullite and SiO_2 according to:

$$3(2SiO_2 \cdot Al_2O_3) \rightarrow 3Al_2O_3 \cdot SiO_2 + 4SiO_2 \qquad (2)$$

A possible further reaction mechanism is given by Higgens and Hendry [2, 3]. This mechanism comprises the formation of SiC from the SiO_2 and finally the formation of β'-sialon from the mullite and SiC:

$$SiO_2 + 3C \rightarrow SiC + 2CO \qquad (3)$$

$$3Al_2O_3 \cdot 2SiO_2 + 4SiC + 3C + 5N_2 \rightarrow 2Si_3Al_3O_3N_5 + 7CO \qquad (4)$$

The quality of the β'-sialon is strongly affected by the exact composition of the raw material and reaction parameters such as temperature, time and nitrogen flow [4–8].

In this paper the reaction mechanism and the influence of the parameters mentioned above are studied in detail.

2. Experimental details

A part of the experiments was performed with spherical pellets of diameter ranging from 2 to 4 mm. These pellets were produced by mixing the kaolin M (see Table I) and carbon (Elftex 125, Cabot) with water in an Eirich mixer (Labormischer RO2). To accelerate the carbothermal reaction $CaCO_3$ was added [9]. The pellets were obtained by sieving. After drying the composition was 79.5 wt % kaolin M, 19.1 wt % carbon and 1.4 wt % $CaCO_3$.

The other experiments were carried out with cylindrical tablets of diameter 13 mm and height ca. 4 mm. These tablets were produced by slipcasting the wet-mixed powders. The compositions of the tablets varied in ratio as well as in type of raw materials. The compositions of the raw materials are given in Table I. All experiments were performed in a horizontal tube furnace. The pellets were placed in an alumina tube (diameter, $D = 25$ mm) in a packed bed (42 g) of about 80 mm long. The tablets were put in an Al_2O_3 boat and then placed in the furnace tube. During the whole experiment nitrogen gas (with 6000 p.p.m. O_2) flowed through the tube at a controlled flow rate (50–400 ml min^{-1} at normal temperature and pressure). The compositions of the reaction products at different stages of reaction were examined by X-ray diffraction (XRD). The quantitative calculations were in accordance with the adiabatic principle of XRD analysis of mixtures [10–12]. The residual carbon content was determined by the weight loss after firing at 650° C in air. Nitrogen analysis of the reacted powders was carried out using boric acid after digestion with LiOH. The reaction progress was followed by monitoring the concentration of the carbon monoxide in the exhaust gas (IFC/GFC gas analyser, Defor, Maihak).

3. Results and discussion

3.1. Influence of time and temperature on the reaction

The influence of time and temperature on the reaction were determined by varying the reaction time from 0 to 16 h for pellets treated at 1400 and 1500° C. The compositions of the reaction products are given in

0022-2461/90 $03.00 + .12

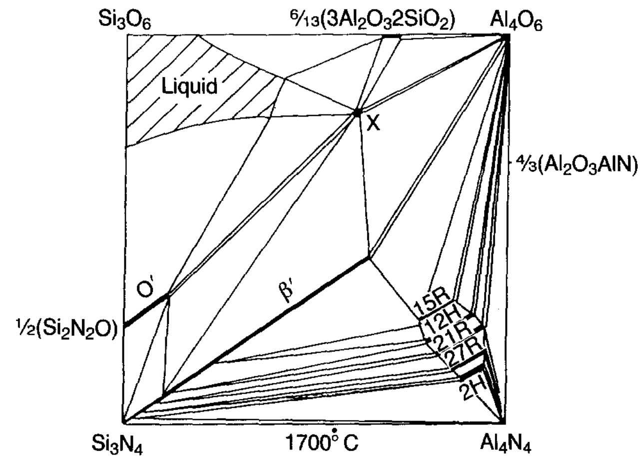

Figure 1 Phase diagram of the system Si_3N_4-Al_2O_3-SiO_2-AlN at 1700°C [1].

Figs 2 and 3. Note that the amount of residual carbon plus the crystalline content is set to 100%, as the amount of amorphous phase (approximately between 20 and 40 wt%) is neglected.

The reaction intermediates at 1400 and 1500°C are the same, though as expected the reaction is faster at 1500°C. In both cases, the maximum β'-sialon content is about 80 wt%. The other compounds in the end product are 15R-phase, β-SiC and Al_2O_3. The presence of 15R-phase indicates an excess of carbon [4, 8]. Another explanation for the presence of 15R is given by Higgens and Hendry [3]. They state that calcium and magnesium impurities result in overnitriding and the formation of 15R on prolonged heating. The stoichiometric starting mixture of kaolin M and carbon black should be 18.8 wt% carbon and 81.2 wt% kaolin. A surplus of 0.3 wt% carbon was added to account for the reduction of impurities and the $CaCO_3$ addition but is evidently too much.

Lee and Cutler [4] report the formation of SiC above a reaction temperature of 1450°C. Carbothermal production of β'-sialon was only successful below this temperature. Van Dijen *et al.* [13] also report the formation of SiC above 1450°C, but only if sufficient carbon is present to remove all the oxygen. In the experiments described in this paper the sialon formation at 1500°C was similar to that at 1400°C. There was no evidence of a process with mainly SiC formation at a reaction temperature of 1500°C.

TABLE I Composition of the minerals used in experiments (wt%)

	NZ[a]	P[b]	M[c]	Al_2O_3[d]	SiO_2[e]	Mullite[f]
Al_2O_3	34.78	33.47	40.35	> 99.6	0.045	72.9
SiO_2	47.36	44.96	43.10	0.03	99.8	24.9
Fe_2O_3	0.3	1.86	0.33	0.03	0.008	0.7
MgO	0.005	0.22	0.01	0.001	0.01	0.2
CaO	0.008	0.62	0.03	0.02		0.2
Na_2O	0.05	0.04	0.03	0.1	0.01	0.3
K_2O	0.007	0.15	0.06			0.7
MnO	0.001	0.003	0.001			
P_2O_5	0.09	0.18	0.09			
TiO_2	0.08	2.14	1.67		0.02	0.1
LOI	15.2	15.2	13.9	< 0.5	0.05	
d_{50} (μm)	0.5	–	2.0	0.5	2.5	
BET ($m^2 g^{-1}$)	20.0	45.2	6.7	3.5	–	–

–: not determined.
[a] From New Zealand Halloysite, China Clays Ltd.
[b] From Provins kaolin, Denain Anzin.
[c] From Monarch kaolin, Cyprus Industrial Minerals Company.
[d] From CT3000, Alcoa.
[e] Milled sand, Sibelco Mam 1 special.
[f] K-REF sintered mullite, Sphinx.
LOI: loss on ignition

The CO content was measured during two experiments. The recordings are given in Fig. 4. Note that in the figures of CO curves $t = 0$ denotes the time when the furnace is switched on; the maximum temperature is reached after ca. 3 h. Fig. 4 shows the first release of CO at about 800°C. This is due to the decomposition of $CaCO_3$ according to:

$$CaCO_3 + C \rightarrow CaO + 2CO \qquad (5)$$

The CO release between 1000°C and 1100°C is probably due to the formation of SiC (Equation 3). The maximum CO content is recorded on reaching the reaction temperature. At 1400°C the CO content is constant after a small drop. This steady-state situation might be related to the movement of the reaction zone through the bed. The presence of a reaction zone is

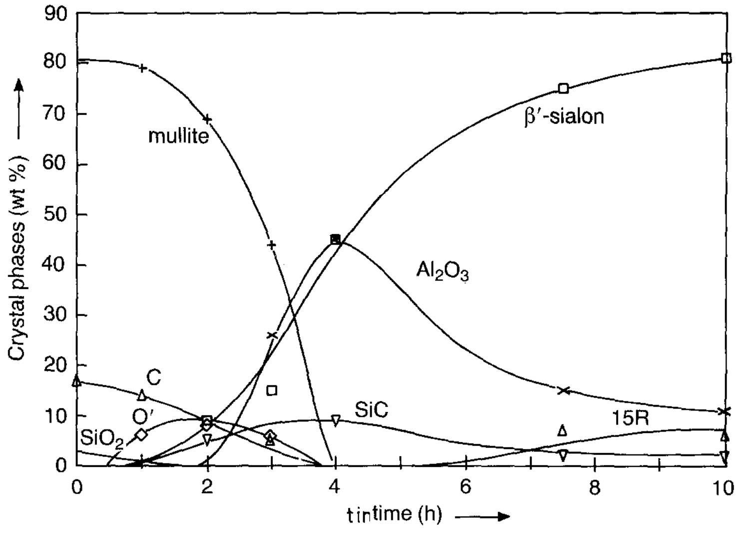

Figure 2 Compositions of the reaction products as a function of the reaction time at 1400°C.

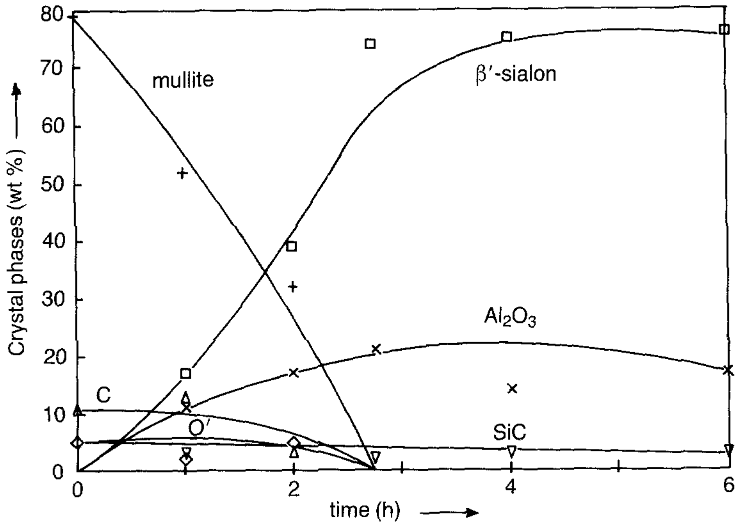

Figure 3 Compositions of the reaction products as a function of the reaction time at 1500° C.

proved by the clear distinction of a zone with reacted and unreacted pellets in a bed. The presence of a reaction zone is also noticed by Spacie [6]. At 1500° C such a period of steady CO flow is absent. This indicates that the reaction is too fast for the formation of a reaction zone moving through the bed. A more detailed study on the kinetics of the reaction mechanism has been carried out by van Neerven [14]. He has described the sialon formation from kaolin using the grain model and discussed the reaction rate limiting processes. In the Figs 2 and 3 it can be seen that the free carbon has disappeared after reaction times of 4 and 3 h at, respectively, 1400 and 1500° C. Taking the heating time into account, this means that in Fig. 4 the CO output after 7.5 and 8.5 must be due to reactions in which no free carbon is involved.

3.2. Reaction mechanism

At the beginning of the reaction (see Figs 2 and 3) some O'-phase is formed which disappears at the same time as the mullite and carbon. At this reaction time the Al_2O_3 content reaches a maximum. Possible reactions responsible for the presence of O', 15R and Al_2O_3 are:

$$2SiO_2 + 3C + N_2 \rightarrow Si_2N_2O + 3CO \tag{6}$$

$$2N_2 + 3Si_2N_2O + 3Al_2O_3 + 6C \rightarrow 6C \rightarrow 2Si_3Al_3O_3N_5 + 6CO \tag{7}$$

$$2SiO_2 \cdot 3Al_2O_3 + 6C \rightarrow 2SiC + 3Al_2O_3 + 4CO \tag{8}$$

$$7SiC + 5Al_2O_3 + 7N_2 \rightarrow SiAl_4O_2N_4 + 2Si_3Al_3O_3N_5 + CO \tag{9}$$

$$3(2SiO_2 \cdot 3Al_2O_3) + 15C + 5N_2 \rightarrow Si_3Al_3O_3N_5 + 6Al_2O_3 + 15CO \tag{10}$$

$$2SiO_2 \cdot 3Al_2O_3 + 2C \rightarrow 2SiO + 2CO + 3Al_2O_3 \tag{11}$$

The formation of SiC, SiO_2 and β'-sialon are given in Equations 2 to 4. Reactions 8 to 10 and 4 have been studied separately. The results of these experiments are given in Table II.

As expected β'-sialon is formed in all four cases. The SiC/Al_2O_3 tablet also contained 15R as reaction product. This is in agreement with Equation 9. The large amount of residual Al_2O_3 in combination with the absence of residual SiC is not fully understood. Possible explanations are the evaporation of SiO (Equation 11) from the mullite and a low reactivity of Al_2O_3. A low reactivity of the used Al_2O_3 is confirmed by a long reaction time of 20 h and the low CO content during the reaction (see Fig. 5). Analysis of the experiment with the mullite/SiC tablet gives a β'-sialon to Al_2O_3 mole ratio of 6 : 19. With the original tablet composition of 50 mol % mullite and 50 mol % SiC

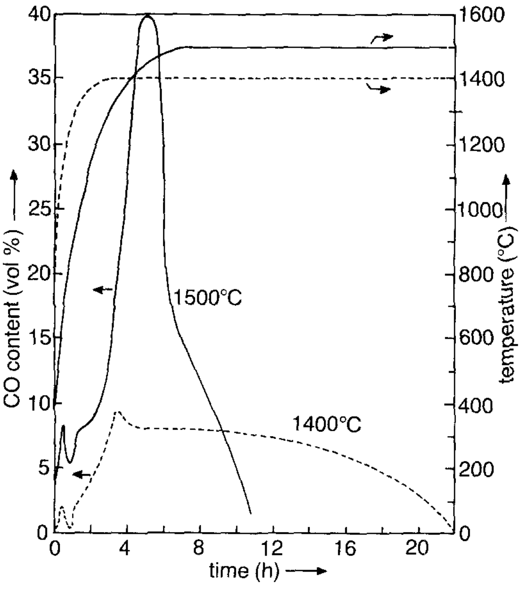

Figure 4 The CO content (in vol %) of the exhaust gas stream during carbothermal reduction at 1400 and 1500° C. For both reactions the heating curves are indicated.

TABLE II Reaction products (in wt %) of some slipcasted tablets reacted at 1400° C in a nitrogen flow of 200 ml min^{-1}

Starting composition	β'-sialon	Al_2O_3	15R	Mullite	SiC
20 SiC, 80 Al_2O_3	16	75	9	–	–
88 mullite, 12 SiC	17	19	–	64	–
68 mullite, 26 SiC, 6 C	53	35	–	4	8
90 mullite, 10 C	24	69	–	7	–

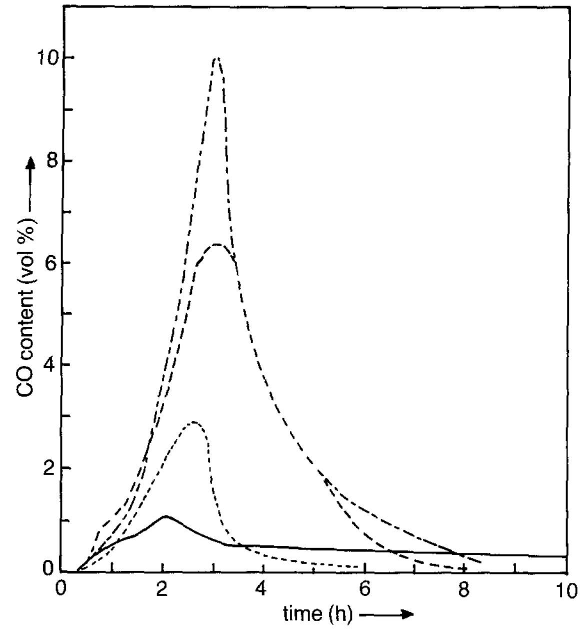

Figure 5 The CO content (in vol %) of the exhaust gas stream during carbothermal reduction at 1400° C of Al_2O_3 + SiC (——), mullite + SiC (····), mullite + C (– – –), mullite + SiC + C (–·–·–·–).

the results can be explained by assuming the following reaction:

$$9(SiO_2 \cdot 3Al_2O_3) + 18SiC + 10N_2 \rightarrow 4Si_3Al_3O_3N_5 + 21Al_2O_3 + 24SiO + 18CO \tag{12}$$

This reaction implies the formation of a large amount of volatile SiO. Part of the SiO can react again, but another part may be removed with the gas stream. Analyses of the condensation products in the cold zone proved the presence of SiO, however, it was not possible to make an appropriate estimation of the degree of evaporation. The amount of SiO loss is further determined by the N_2 flow rate and the reaction temperature.

3.3. The influence of N_2 flow and pellet size

The influence of flow and pellet size is studied by two series of experiments at 1500° C: one with pellets ranging from 2 to 4 mm and one with pellets ranging from 0.8 to 2 mm. Each series consisted of a number of experiments performed at different flows with a reaction time of 2 h. The crystalline phase content of the reaction products was analysed by XRD. The results are given in Fig. 6. This figure shows that there is no significant difference between the experiments with the pellets ranging from 0.8 to 2 mm and those ranging 2 to 4 mm. Apparently, under the given process circumstances, this variation of pellet size does not influence the reaction rate.

The influence of the pellet size is also measured with two experiments at 1400° C. The CO curves of these experiments are given in Fig. 7. In this case, the small pellets show a much larger reaction rate than the large pellets. The CO curve of the small pellets no longer shows a period of steady CO flow. These experiments explain the apparent disagreement between results reported in the literature by Higgens and Hendry [3] and van Dijen and Metselaar [5]. Higgens and Hendry [3] measured the CO flow during the reaction with a nitrogen flow of 400 ml min^{-1} and 1450° C and did not notice any difference between pellets of 1.5 or 3.5 mm. On the other hand, van Dijen and Metselaar [5] claim an influence of the pellet size on the reaction rate at 1400° C. The difference between the results in Figs 6 and 7 can be explained by the reaction temperature.

At a high reaction temperature (1500° C) a decrease of the pellet size below 4 mm has no influence on the reaction rate. At a lower reaction temperature (1450° C) a decrease of the pellet size from the range 2 to 4 mm to the range 0.8 to 2 mm does increase the reaction rate. Apparently for each reaction temperature a critical pellet diameter can be determined. Decreasing the diameter below this critical diameter has no influence on the reaction rate, however, a higher reaction temperature will have a larger critical pellet diameter. It is important to note that an increase of temperature causes an increase in the gas velocity. It might well be possible that a change in gas velocity causes a change in the critical pellet diameter.

Fig. 6 shows a strong relation between the reaction rate and the flow. An increase in the flow increases the reaction rate. At a flow of 400 ml min^{-1} the conversion after 2 h is equal to the conversion after 6 h at 100 ml min^{-1}. A disadvantage of a higher flow is the formation of more 15R; after 2 h at 400 ml min^{-1} the reaction product contained 80 wt % sialon and 17 wt %

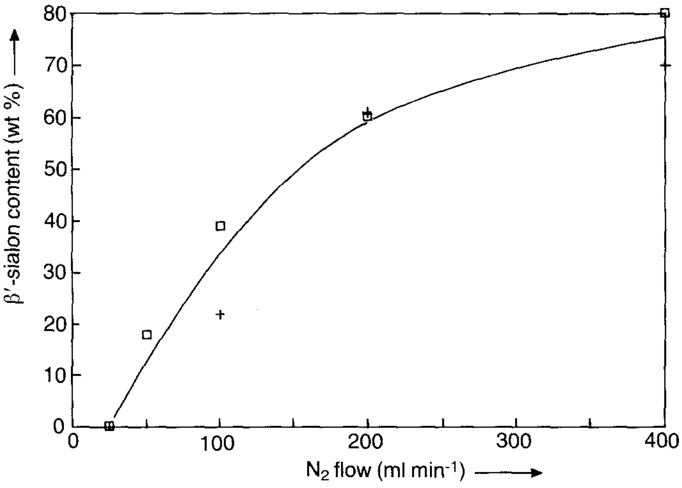

Figure 6 The β'-sialon content of the reaction products after a reaction time of 2 h at 1500° C as function of nitrogen flow role for pellet size fractions of 0.8–2 mm (□) and 2–4 mm (+).

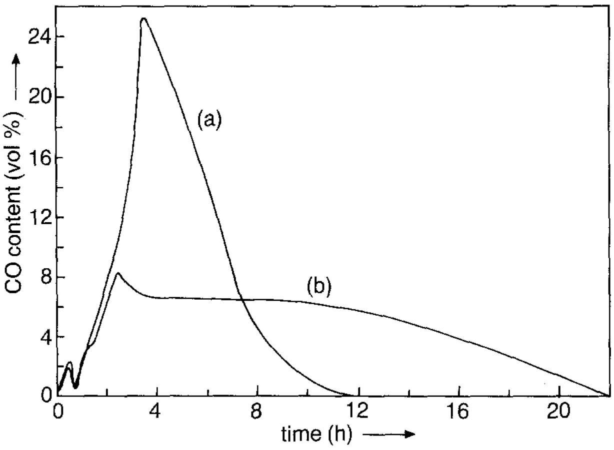

Figure 7 The CO content (in vol %) of the exhaust gas stream during carbothermal reduction at 1400° C for two different pellet size fractions.

15R, whereas, after 6 h at 100 ml min^{-1} the product contained 81 wt % sialon and 8 wt % 15R. A possible explanation is the higher loss of SiO due to the higher flow. A higher SiO loss might promote the formation of Al-richer 15R phase above that of β'-sialon. The influence of the flow was also measured with the following CO-monitoring experiment.

The CO curves of the experiments at 1400° C show a period of constant CO content (see Fig. 4). If during this period the gas flow is varied the CO level will change. In Fig. 8 the change of the CO level is measured as function of flow. Dilution by the higher flow will cause a lowering of the CO level at higher flows. If the CO flow (in mmol h^{-1}) is plotted instead of the CO percentage it can be seen that the CO content increases at higher flows. Since a higher CO flow indicates a higher reaction rate it can be stated that an increase in the nitrogen flow increases the reaction rate. At very high nitrogen flows (> 500 ml min^{-1}) the influence on the reaction rate becomes very small. Van Dijen *et al.* [8] recommend a low nitrogen flow to prevent the formation of a mixture of Si_3N_4 and AlN instead of β-sialon, due to SiO loss.

Van Dijen *et al.* [5, 9] described the influence of flow and pellet size by the Reynolds number (*Re*):

$$Re = \frac{\beta_g v_g d_p}{\mu_g} \qquad (13)$$

where ϱ_g is the gas density, v_g the superficial gas velocity, d_p the pellet diameter and μ_g the dynamic viscosity of the gas. They stated that for $Re < 0.05$, mass transfer (film diffusion) must be rate determining and that pore diffusion can be neglected up to a pellet diameter of 2 mm. Under these conditions the reaction rate in a packed bed with porosity of 40% is proportional to $d_p Re^{-1/3}$. For $Re > 0.05$ the chemical reaction becomes the rate-controlling step. Clearly this description with *Re* is not able to explain the experiments that show no influence from pellet size.

As mentioned above, at each temperature there is a critical pellet size below which the reaction becomes independent of the pellet diameter. Van Neerven [14] has shown that this behaviour can be described well by the so-called Szekely grain model [15]. According to this model the reaction rate is the sum of two terms, one determined by the chemical reaction rate, the other by the pore diffusion rate. Important factors in this model are the pellet diameter d_p and the modified Sherwood number Sh^*. For small pellet size and large Sh^* the chemical kinetics are rate determining. Experiments at 1400° C showed that pore diffusion can be neglected for $d_p < 1$ mm. In contradiction with van Dijen, van Neerven assumed that Sh^* is too large to cause external mass transfer resistance under conditions where pore diffusion can be neglected. For the pellet fraction of size from 2 to 4 mm (used for this study) at 1400° C pore diffusion cannot be neglected.

3.4. Influence of the composition

The composition of the starting mixture has a great influence on the reaction mechanism and reaction times. First the influence of the amount of carbon in kaolin M-carbon mixtures at 1500° C is studied. After a reaction time of 2 h the composition was determined by XRD (see Fig. 9). As can be seen in this figure an excess of carbon decreases the amount of β'-sialon formed after 2 h. A large excess of carbon (3 wt %) leads to the formation of Si_3N_4. This is in agreement with van Dijen *et al.* [8]. For complete conversion a stoichiometric amount of carbon (i.e. 18.9 wt %) is necessary. This means that the best results will be achieved with a stoichiometric amount of carbon. A slight shortage of carbon is usually connected in the literature with the formation of X phase and Al_2O_3

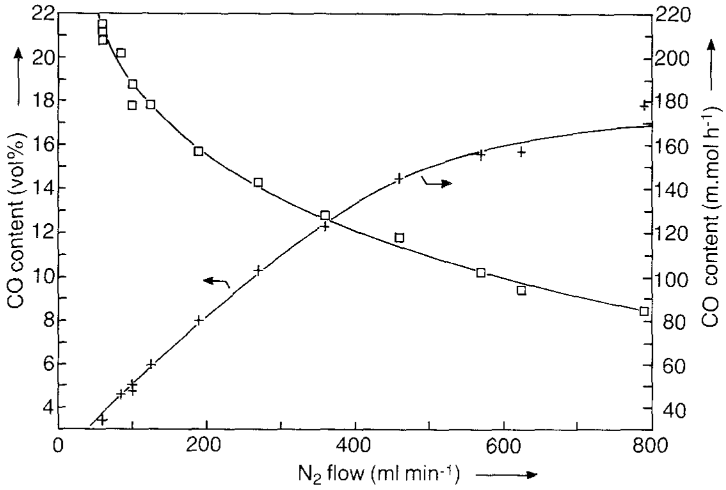

Figure 8 The influence of nitrogen flow on the CO content in the exhaust gas stream during carbothermal reduction at 1400° C, when the CO level has reached a stationary value. The CO content is given in vol % of the exhaust gas stream and in mmol h^{-1}.

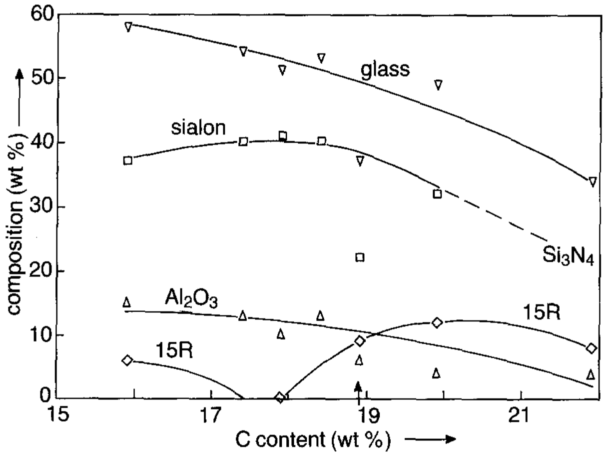

Figure 9 The influence of the carbon content on the compositions of the reaction products of carbothermal reduction after 2 h at 1500° C. The arrow at 18.8 wt % indicates the stoichiometric carbon content.

TABLE III The composition of the reaction products (in wt %) of experiments with different additives

Additive		Glass	Sialon	Al_2O_3	15R	Other
MgO	1	39	29	–	–	$MgAl_2O_4$ 25; mullite 7
	2	40	25	–	–	34
	6	31	29	–	–	40
Fe_2O_3	1	43	25	7	–	Fe_2Si 0.7; Si_3N_4 24
	2	30	27	11	–	1.0; 31
	6	44	27	–	–	1.6; 28
$CaCO_3$	1	21	59	14	5	–
	2	29	59	5	7	–
	6	58	30	–	11	–
Y_2O_3	1	27	45	19	2	YAG 7
	2	20	43	21	1	15
	6	16	24	24	–	30
TiO_2	1	57	27	–	–	mullite 13; TiN 3
	2	58	33	4	–	0; 1
	6	60	27	4	–	7; 2
None*		61	28	7	4	–

*cf. Table I for the impurities present in the kaolin M.

[4, 6, 7] but no X phase was detected in the reaction products in Fig. 10. Another explanation for the appearance of X is given by Higgens [2]. He suggests that X-phase is formed if potassium is present as an impurity whereas O′ is formed if calcium is present.

The influence of additives on the reaction and reaction products of a mixture of kaolin M and carbon was studied by CO-monitor experiments. The experiments were carried out using slipcasted tablets at 1400° C and a nitrogen flow of 200 ml min^{-1}. The size and porosity of pellets and tablets are different. Therefore, the compositions of the reaction products of both cannot be compared. The reaction products were analysed by XRD and the results are given in Table III.

As shown in Table I the main natural impurities in this clay are Fe_2O_3 (0.33 wt %) and TiO_2 (1.67 wt %). These impurities result in traces of TiN and Fe_2Si in all the reaction products (these traces are not mentioned in Table III). MgO, Fe_2O_3, $CaCO_3$, Y_2O_3 and TiO_2 were used as additives. The addition of 1 wt % $CaCO_3$ results in the highest amount of β'-sialon (59 wt %) and a high amount of crystalline phase (79 wt %). Y_2O_3 addition results in a high amount of crystalline phase but besides β'-sialon, alumina and yttrium aluminium garnet (YAG) are also formed. MgO, Fe_2O_3 and TiO_2 additions increase the glass phase content and decrease the β'-sialon content of the reaction product. Fe_2O_3 promotes the formation of β-Si_3N_4 instead of β'-sialon. Higgens [2] also reported that Fe_2O_3 lowers the z-value of the produced sialon. An increasing amount of Y_2O_3 and MgO results in an increase of the amount of crystalline phase. Only the addition of Fe_2O_3 has a strong influence on the reaction rate. The total reaction time is reduced from 11 to 6 h while the other mixtures had a reaction time of about 9 h (see Fig. 10).

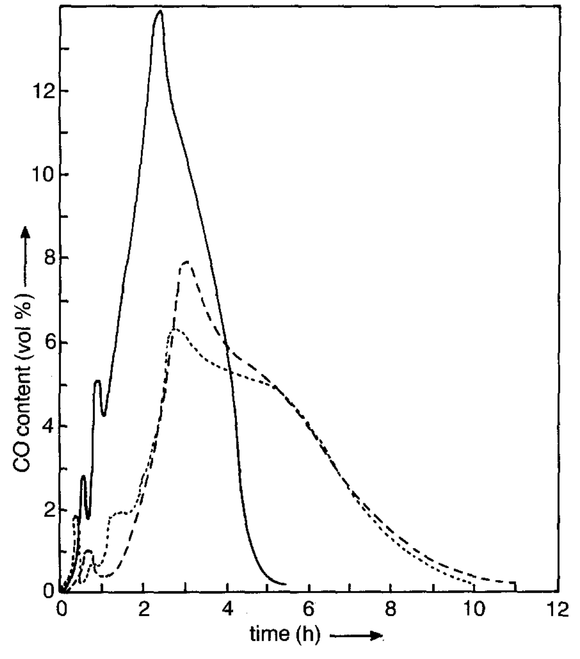

Figure 10 The CO content (in vol %) of the exhaust gas stream during carbothermal reduction at 1400° C for various additives. (——) 6 wt % Fe_2O_3, (– – –) no additive, (· · ·) 6 wt % $CaCO_3$.

The influence of some clay types was studied. The reaction of three different kaolins and of a mixture of SiO_2 and Al_2O_3 was studied by a CO-monitor experiment (Fig. 11). The three clays differ in composition as well as in morphology (see Table I). The CO monitorings show a very fast reaction for kaolin P and the slowest reaction for the mixture of Al_2O_3 and SiO_2. Kaolin M reacted faster than kaolin NZ. The compositions of the reaction products of the four experiments are given in Table IV.

It is clear that kaolin P not only reacts very fast but also leads to the largest amount of crystalline β'-sialon. Kaolin NZ yields a considerable amount of Si_3N_4 while the reaction product of the Al_2O_3/SiO_2 mixture contains a lot of Al_2O_3. Explanations for the results with kaolin P lie in the very fine particle size

TABLE IV Composition of the reaction products (in wt %) of experiments with different SiO_2/Al_2O_3 sources

	Sialon	Al_2O_3	15R	Si_3N_4	Glass
M kaolin	31	7	4	–	57
P kaolin	59	–	–	–	40
NZ kaolin	29	–	5	19	47
SiO_2/Al_2O_3	21	14	–	–	65

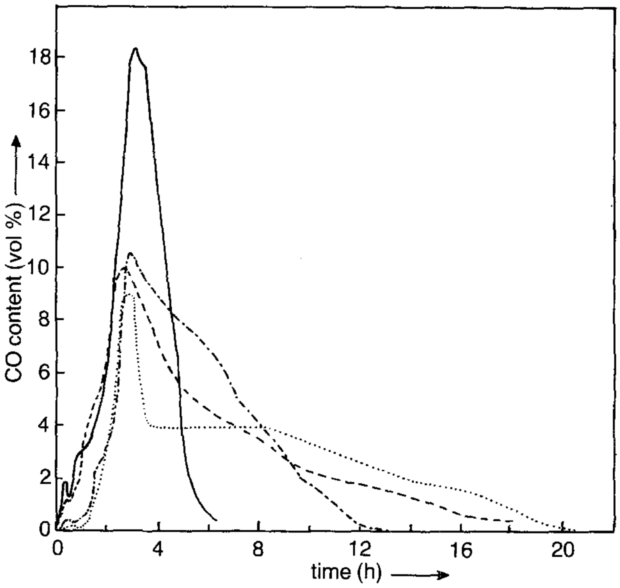

Figure 11 The CO content (in vol %) of the exhaust gas stream during carbothermal reduction of different SiO_2/Al_2O_3 sources at 1400° C (cf. Table I). (——) P, (– – –) NZ, (–·–·–) M, (· · ·) Al_2O_3/SiO_2.

and the presence of a relatively large amount of Fe_2O_3 (1.8 wt %) and CaO (0.65 wt %). The slow reaction of the mixture of SiO_2 and Al_2O_3 will be due to the relatively bad mixing of the compounds compared to the molecular mixing within the kaolins and the purity of the minerals. Because of the absence of impurities no liquid phase will be formed which would accelerate the reaction. The difference between the kaolins NZ and M is possibly due to the purity of the kaolin NZ which causes a somewhat slower reaction. A reason for the formation of Si_3N_4 is not found.

4. Conclusions

The carbothermal reduction of kaolin at 1400 and 1500° C takes place according to the same reaction mechanism. In both cases the same phases are formed: Al_2O_3, O′, mullite, SiC, 15R and β'-sialon. The formation of β'-sialon from the intermediate phases is confirmed by the experiments.

An increase in the nitrogen flow causes an increase in the reaction rate. Under the conditions of constant flow, at each reaction temperature a critical pellet size can be determined below which a further decrease of the size has no influence on the reaction rate. This critical pellet size increases with increasing temperature.

The best results are obtained with a stoichiometric amount of carbon. An excess of carbon decreases the amount of β'-sialon. Additives and impurities influence the conversion and reaction rate. Of the additives studied only Fe_2O_3 increases the reaction rate. Unfortunately Fe_2O_3 decreases the amount of β'-sialon formed and leads to formation of Fe_2Si. The highest yield of β'-sialon is obtained by addition of 1 wt % $CaCO_3$.

The SiO_2/Al_2O_3 source also has a great influence on the reaction. Not only the composition, i.e. the purity of the material, but also the morphology (e.g. particle size) influences the reaction rate and final composition.

Acknowledgements

The investigations were supported in part by the Innovative Research Program Technical Ceramics (IOP).

References

1. W. Y. SUN and D. S. YAN, *Rev. Solid State Sci.* **1** (1988) 493.
2. I. HIGGENS, PhD thesis, University of Newcastle upon Tyne (1986).
3. I. HIGGINS and A. HENDRY, *Brit. Ceram. Trans. J.* **85** (1986) 161.
4. J. G. LEE and I. B. CUTLER, *Ceram. Bull.* **58** (1979) 869.
5. F. K. VAN DIJEN and R. METSELAAR, *J. Amer. Ceram. Soc.* **68** (1985) 16.
6. C. J. SPACIE, private communication.
7. F. K. VAN DIJEN, R. METSELAAR and C. A. M. SISKENS, *Fortschritte deutsch. keram. Gesellschaft* **1** (1985) 113.
8. F. K. VAN DIJEN, C. A. M. SISKENS and R. METSELAAR, in Proceedings of the 12th International Conference on Science of Ceramics 12, Saint-Vincent, June 1983, edited by P. Vincenzini (Grafiche Galeati, Imola, 1984) p. 427.
9. F. K. VAN DIJEN, PhD thesis, Eindhoven University of Technology (1986).
10. F. H. CHUNG, *J. Appl. Cryst.* **7** (1974) 519.
11. *Idem, ibid.* **7** (1974) 526.
12. *Idem, ibid.* **8** (1975) 17.
13. F. K. VAN DIJEN, R. METSELAAR and C. A. M. SISKENS, *Sprechsaal* **117** (1984) 627.
14. A. M. VAN NEERVEN, MSc thesis, Centre for Technical Ceramics, Eindhoven University of Technology (1988).
15. J. SZEKELY, J. W. EVANS and H. Y. SOHN, "Gas-Solid Reactions" (Academic Press, New York, 1976).

Received 6 October 1988
and accepted 28 February 1989